INFECTION AND IMMUNITY, May 1997, p. 1659–1668 Vol. 65, No. 5
0019-9567/97/$04.00+0

Genetic Organization of the Yersiniabactin Biosynthetic Region and Construction of Avirulent Mutants in *Yersinia pestis*

SCOTT W. BEARDEN, JACQUELINE D. FETHERSTON, AND ROBERT D. PERRY*

Department of Microbiology and Immunology, University of Kentucky, Lexington, Kentucky 40536-0084

Received 8 October 1996/Returned for modification 15 January 1997/Accepted 5 February 1997

We have identified an ~22-kb region of the *pgm* locus of *Yersinia pestis* KIM6+ which encodes a number of iron-regulated proteins involved in the biosynthesis of the *Y. pestis* cognate siderophore, yersiniabactin (Ybt), and which is located immediately upstream of the pesticin/yersiniabactin receptor gene (*psn*). Sequence analysis and the construction of insertion and deletion mutants allowed us to determine the putative location of the *irp1* gene and the positions of *irp2*, *ybtT*, and *ybtE* within the *ybt* operon. Mutations in the *irp1*, *irp2*, or *ybtE* gene yielded strains defective in siderophore production. Mutant strains were unable to grow on iron-deficient media at 37°C but could be cross-fed by culture supernatants from yersiniabactin-producing strains of *Y. pestis* grown under iron-limiting conditions. Sodium dodecyl sulfate-polyacrylamide gel electrophoresis analysis of whole-cell extracts from Ybt^+ and Ybt^- strains grown in iron-deficient media revealed that expression of *ybt*-encoded proteins is not only iron regulated but also influenced by the presence of the siderophore itself. Finally, *Y. pestis* strains with mutations in either the *psn* or *irp2* gene were avirulent in mice when inoculated subcutaneously.

Iron, with few exceptions, is an essential element of all living cells. Yet despite its abundance in nature, it remains largely inaccessible in aerobic, aqueous environments at neutral pH, where it forms stable polymers of sparingly soluble ferric hydroxides and oxyhydroxides (25). Iron serves as an essential cofactor in a number of enzymatic and metabolic reactions (24). Among bacterial pathogens, the successful establishment of disease in a mammalian host is dependent on the ability of the invading organism to acquire iron. In mammalian systems, iron is confined mostly to intracellular compartments as metalloprotein complexes such as hemoglobin, myoglobin, and ferritin (40). The high-affinity iron-binding glycoproteins transferrin and lactoferrin sequester the trace amounts of iron found in the extracellular milieu, limiting the amount of free iron in vertebrate fluids to $\sim 10^{-18}$ M (38, 40). Since this value is dramatically below the level of iron required for optimal microbial growth, low-molecular-weight ferric iron chelators, termed siderophores, are used by many bacteria to overcome the challenges of iron deficiency (4). Siderophores display considerable variation in their structures but are generally classified as either hydroxamates such as aerobactin or catecholates exemplified by enterobactin (14). Expression of these compounds is often negatively regulated by Fur, a DNA-binding protein that, when complexed with ferrous iron, tightly adheres to operator sequences of genes under its regulation (15).

The correlation between iron availability and virulence is well established for *Yersinia pestis*, the etiologic agent of bubonic plague (44). This was first demonstrated in spontaneous nonpigmented (Pgm^-) mutants of *Y. pestis* in which virulence in mice was restored when these strains were supplemented with hemin or inorganic iron prior to inoculation from peripheral routes (32). The Pgm^+ phenotype was originally defined not only as the ability of *Y. pestis* to form dark brown or pigmented colonies when grown at 26°C on solidified media containing hemin but also as iron-independent virulence in mice (32, 33). The Pgm^+ phenotype includes: (i) sensitivity to the bacteriocin pesticin in strains lacking the pesticin plasmid pPCP1 (5); (ii) growth at 37°C in an iron-chelated, defined medium (20, 54); (iii) expression of the gene (*psn*) encoding the receptor for pesticin (21, 55) and of the iron-regulated genes *irp1* and *irp2*, encoding proteins of 240 kDa (HMWP1) and 228 kDa (HMWP2), respectively (8, 21, 26); and (iv) yersiniabactin biosynthesis (20). Formation of colored colonies in *Y. pestis* is a manifestation of the hemin storage locus (*hms*), an approximately 7-kb region unique to Pgm^+ strains that encodes proteins capable of restoring temperature-regulated adsorption of hemin or Congo red (CR) to Pgm^- deletion mutants (43, 46, 61). Providing the *hms* locus to nonpigmented strains in *trans*, however, did not result in a concomitant restoration of pesticin sensitivity or expression of iron-regulated proteins HMWP1 and HMWP2 and the pesticin receptor (Psn). Genetic evidence has demonstrated that loss of all Pgm^+ traits commonly occurs via the spontaneous deletion of a 102-kb segment of the *Y. pestis* chromosome referred to as the pigmentation (*pgm*) locus (22). Loss of the Pgm^+ phenotype occurs at a frequency of $\sim 10^{-5}$ and is thought to be mediated by the presence of a repetitive element found at both ends of the locus (5, 21, 22).

Indirect evidence for siderophore production by *Y. pestis* has been previously reported (65), and synthesis of the siderophore yersiniabactin/yersiniophore (Ybt) has been firmly established in *Yersinia enterocolitica* (10, 17, 27). Purification and elucidation of the structure of Ybt from *Yersinia enterocolitica* has been reported recently and shown to be closely related to pyochelin and anguibactin, siderophores produced by *Pseudomonas aeruginosa* and *Vibrio anguillarum*, respectively (10, 17, 27). Although the genes required for biosynthesis of Ybt have not been conclusively determined, Guilvout et al. (26) have reported that the *irp2* gene of *Y. enterocolitica* encoding the 228-kDa HMWP2 protein exhibits extensive homology to a large family of adenylate-forming enzymes involved in the biosynthesis of peptide antibiotics and siderophores. Chambers and Sokol (11) demonstrated that siderophore production by enteropathogenic *Yersinia* spp. correlated with the expression of HMWP2 and the 240-kDa protein, HMWP1. An *irp2*::*kan* mutation in *Y. pestis* resulted in loss of a growth-stimulatory

* Corresponding author. Phone: (606) 323-6341. Fax: (606) 257-8994. E-mail: rperry@pop.uky.edu.

TABLE 1. Bacterial strains and plasmids used[a]

Strain or plasmid	Relevant characteristics	Source or reference
Y. pestis		
KIM5-2045.21	*hms*$^+$ Psn$^-$ (Δ*psn2045.1*) *irp1*$^+$ *irp2*$^+$ *ybtE*$^+$ Ybt$^+$ Psa$^-$ (Δ*psa2053.1*) Lcr$^+$ [pCD1::Mu*d*I1734-73 (*yopJ*::Mu*d*I1734)] Km^r; derived from KIM6-2045.2	This study
KIM5-2046.41	*hms*$^+$ *psn*$^+$ Ybt$^-$ (Δ*irp2-2046.3*) Psa$^-$ (Δ*psa2053.1*) Lcr$^+$ [pCD1::Mu*d*I1734-73 (*yopJ*::Mu*d*I1734)] Km^r; derived from KIM6-2046.4	This study
KIM5-2053.11+	*hms*$^+$ *psn*$^+$ Psa$^-$ (Δ*psa2053.1*) Ybt$^+$ Lcr$^+$ [pCD1::Mu*d*I1734-73 (*yopJ*::Mu*d*I1734)] Km^r; derived from KIM6-2053.1+	This study
KIM6+	*hms*$^+$ *psn*$^+$ *irp1*$^+$ *irp2*$^+$ *ybtE*$^+$ Psa$^+$ Ybt$^+$ Lcr$^-$	54
KIM6-2045.1	*hms*$^+$ Psn$^-$ (Δ*psn2045.1*) *irp1*$^+$ *irp2*$^+$ *ybtE*$^+$ Psa$^+$ Ybt$^+$ Lcr$^-$	20
KIM6-2045.2	*hms*$^+$ Psn$^-$ (Δ*psn2045.1*) *irp1*$^+$ *irp2*$^+$ *ybtE*$^+$ Ybt$^+$ Psa$^-$ (Δ*psa2053.1*) Lcr$^-$; derived from KIM6-2053.1+	This study
KIM6-2046.1	*hms*$^+$ *psn*$^+$ Psa$^+$ Ybt$^-$ (*irp2*::*kan2046.1*) HMWP1$^-$ YbtE$^-$ Lcr$^-$ Km^r	20
KIM6-2046.2	*hms*$^+$ *psn*$^+$ *irp2*::pCSIRP498.9 Psa$^+$ Ap^r; derived from KIM6+	This study
KIM6-2046.3	*hms*$^+$ *psn*$^+$ Psa$^+$ Ybt$^-$ (Δ*irp2-2046.3*) Lcr$^-$; derived from KIM6-2046.2	This study
KIM6-2046.3(pIRP2)	*hms*$^+$ *psn*$^+$ Δ*irp2-2046.3*/*irp2*$^+$ HMWP1$^+$ HMWP2$^+$ Psa$^+$ Ybt$^+$ Lcr$^-$ Km^r Ap^r; derived from KIM6-2046.3	This study
KIM6-2046.4	*hms*$^+$ *psn*$^+$ Ybt$^-$ (Δ*irp2-2046.3*) Psa$^-$ (Δ*psa2053.1*) Lcr$^-$; derived from KIM6-2053.1+	This study
KIM6-2053+	*hms*$^+$ *psn*$^+$ *psa*::pCVDPSA1 Ybt$^+$ Lcr$^-$ Ap^r; derived from KIM6+	This study
KIM6-2053.1+	*hms*$^+$ *psn*$^+$ Psa$^-$ (Δ*psa2053.1*) Ybt$^+$ Lcr$^-$; derived from KIM6-2053+	This study
KIM6-2054.1	*hms*$^+$ *psn*$^+$ Psa$^+$ Ybt$^-$ (*irp1*::*kan2054.1*) HMWP2$^-$ YbtE$^-$ Lcr$^-$ Km^r; derived from KIM6+	This study
KIM6-2056	*hms*$^+$ *psn*$^+$ *ybt*::pCHIRP56.2 Psa$^+$ Lcr$^-$ Ap^r; derived from KIM6+	This study
KIM6-2056.1	*hms*$^+$ *psn*$^+$ Psa$^+$ Ybt$^-$ (Δ*ybtE2056.1*) Lcr$^-$; derived from KIM6-2056	This study
E. coli		
DH5α	Cloning strain; Ybt$^-$	2
SY327(λ*pir*)	Strain for propagating plasmids with R6K origins	41
Plasmids		
pBGL2	4.8-kb cloning vector; Ap^r Tc^r	46
pBluescript II KS+	3.0-kb cloning vector; Ap^r	Stratagene[b]
pCVD442	6.2-kb suicide vector with R6K origin; Ap^r SacB$^+$	16
pUC-4K	pUC vector containing *kan* cassette from Tn*903*; Ap^r Km^r	64
pUC18	2.7-kb cloning vector; Ap^r	51
pCD1::Mu*d*I1734-73	Lcr plasmid derived from pCD1; Lcr$^+$/YopJ$^-$ (*yopJ*::Mu*d*I1734)	60
pCHIRP56.2	3.8-kb *Sph*I/*Sal*I fragment from pHIRP56 and 1.3-kb *Sal*I/*Eco*RV fragment from pPSN4 into pCVD442; Ap^r	This study
pCIRP1	11.6-kb *Sal*I insert from pKIRP1 into pCVD442; Ap^r Km^r	This study
pCSIRP498.9	2.5-kb *Sal*I/*Eco*RV fragment from pSIRP498.9 into vector pCVD442; Ap^r	This study
pCVDPSA1	~4.2-kb *Eco*RI/*Sal*I fragment from pDG6.2 cloned into pCVD442; Ap^r	This study
pDG6	~9-kb *Cla*I fragment containing *psa* locus in vector pHSS6; Km^r	36
pDG6.1	4.8-kb (two *Eco*RI fragments) deleted from *psa* locus of pDG6; Δ*psa* Km^r	This study
pDG6.2	~4.2-kb *Cla*I insert from pDG6.1 cloned into pBluescript II KS$^+$; Ap^r	This study
pHIRP56	984-bp *Hpa*I deletion in pPSN3; Δ*ybtE* Ap^r	This study
pIRP2	9.5-kb *Sal*I fragment encoding *irp2* from pSDR498.8 into pBGL2; Ap^r	21
pKIRP1	1.2-kb *kan* cassette from pUC-4K inserted in *Bst*BI site of pPSN3; Ap^r Km^r	This study
pSDR498.9	3.9-kb *Sal*I/*Bgl*II fragment of pSDR498.3 into pBGL2; Ap^r	This study
pSIRP498.9	471-bp *Ssp*I in-frame deletion fragment in *irp2* derived from pSDR498.9	This study

[a] *Y. pestis* strains with a plus sign possess an intact 102-kb *pgm* locus containing the genes for hemin storage (*hms*), *psn*, *irp1*, *irp2*, *ybtT*, *ybtE*, and *ybtA*. All other *Y. pestis* strains contain a mutation within the *pgm* locus due to either a deletion or insertion of an antibiotic resistance cassette. Strains producing the siderophore yersiniabactin are designated Ybt$^+$, while those defective in yersiniabactin secretion are Ybt$^-$. pCD1::Mu*d*I1734-73 is a derivative of the 75-kb virulence plasmid pCD1 and confers the low-calcium-response (Lcr$^+$) phenotype. The Psa$^+$ phenotype is a product of the pH 6 antigen gene (*psa*). Abbreviations: Ap^r, Km^r, and Tc^r, resistance to ampicillin, kanamycin, and tetracycline, respectively.

[b] Stratagene Cloning Systems, La Jolla, Calif.

activity, presumably mediated by Ybt, necessary for growth at 37°C under iron-deficient conditions (20). Given the near sequence identities of the *irp2* genes and the Ybt/pesticin receptor genes (designated *psn* in *Y. pestis* and *fyuA* in *Y. enterocolitica*) between *Y. pestis* and *Y. enterocolitica* (20, 26, 48), it is likely that the siderophore produced by the plague bacillus is similar if not identical to the high-affinity iron-binding compound secreted by other pathogenic yersiniae (11, 27). Finally, maximal expression of the *Y. pestis* Ybt receptor gene, *psn*, is dependent on the presence of Ybt and an AraC-like activator, YbtA (19, 20).

In this investigation, we have identified a region of the *pgm* locus, approximately 22 kb in size, which encodes a number of iron-regulated polypeptides necessary for the biosynthesis of the *Y. pestis* siderophore, Ybt. We demonstrate the involvement of HMWP2 and a 56-kDa protein designated YbtE in siderophore biosynthesis by *Y. pestis*. Additionally, we show that Hms$^+$ strains of *Y. pestis* with mutations in either the *psn* or *irp2* gene are avirulent in mice when injected subcutaneously.

MATERIALS AND METHODS

Bacterial strains, plasmids, and media. All relevant characteristics of strains and plasmids used in this study are presented in Table 1. All *Y. pestis* strains were derived from KIM6+, which contains the endogenous plasmids pMT1 and pPCP1 (55). KIM6+ lacks the ~75-kb plasmid pCD1 that encodes a number of

essential virulence determinants that are transcriptionally regulated by calcium (6, 22, 46, 55). The potentially virulent *Y. pestis* strains, KIM5-2045.2 (Δ*psn2045.1*), KIM5-2046.4 (Δ*irp2-2046.3*), and KIM5-2053.11+ (Δ*psa2053.1*) containing the pCD1 derivative, pCD1::Mu*d*I1734-73 (*yopJ*::Mu*d*I1734) (60), were used in mouse 50% lethal dose (LD_{50}) experiments described below. The Pgm^+ phenotype of *Y. pestis* strains used for virulence testing in mice was verified by plating onto CR agar (61) containing kanamycin (50 μg/ml), whereas the Lcr^+ phenotype was determined by differential plating onto tryptose blood agar base (TBA; Difco Laboratories) containing kanamycin (50 μg/ml) and 20 mM each $MgCl_2$ and sodium oxalate (30). *Y. pestis* strains were grown on TBA containing ampicillin (50 μg/ml) and kanamycin (50 μg/ml) where appropriate. For experiments requiring growth in liquid culture, *Y. pestis* strains were grown in either heart infusion broth or, for iron-deficient growth, the chemically defined medium PMH which had been extracted prior to use with Chelex 100 resin (Bio-Rad Laboratories) (58). Precipitation of residual iron not removed by the chelating resin in deferrated PMH was achieved by the addition of 0.5 mM $NaCO_3$, 0.01 mM $MnCl_2$, and 4.0 mM $CaCl_2$ (PMH-S). PMH-S plates were solidified with either 1.0% agarose or 1.4% Noble agar and subsequently used in cross-feeding experiments or to determine the growth characteristics of the *ybt* mutants at 37°C as previously described (20). For iron-replete growth, *Y. pestis* strains were cultivated in PMH supplemented with 10 μM $FeCl_3$. *Escherichia coli* strains were grown in either Luria broth (2) or Terrific broth (62) supplemented with ampicillin (100 μg/ml), kanamycin (50 μg/ml), or tetracycline (12.5 μg/ml) when indicated.

Construction of *ybt* mutants. The generation of *Y. pestis* strain KIM6-2046.1 bearing a kanamycin resistance gene (*kan*) cassette in the *irp2* gene encoding the iron-regulated protein HMWP2 has been previously reported (20). For construction of an in-frame deletion in the *irp2* gene, we subcloned a ~3.9-kb *Sal*I/*Bgl*II fragment of plasmid pSDR498.3 (21) into the *Sal*I/*Bgl*II site of the vector pBGL2 (46) to generate pSDR498.9 (Table 1). An examination of the *irp2* nucleotide sequence from *Y. enterocolitica* (26 [Genbank accession number L18881]) enabled us to identify two *Ssp*I restriction sites separated by 471 bp (26) which are conserved in *Y. pestis*. Removal of this *Ssp*I fragment from pSDR498.9 resulted in plasmid pSIRP498.9. pCSIRP498.9 was generated by subcloning a ~2.5-kb *Sal*I/*Eco*RV fragment from pSIRP498.9 into the *Sal*I/*Sma*I sites of the suicide plasmid pCVD442 (16). Introduction of a *kan* cassette into the *irp1* gene of *Y. pestis* was accomplished by ligation of a *kan* gene contained in an *Acc*I fragment from plasmid pUC-4K (64) into the *Bst*BI site of pPSN3 (21). The *Sal*I insert fragment from the resulting plasmid, designated pKIRP1, was subcloned into *Sal*I-digested pCVD442, yielding recombinant pCIRP1 (Table 1). Recombinant pPSN3 was also used to construct a *ybtE* deletion mutant. Removal of a 984-bp *Hpa*I fragment from pPSN3 generated plasmid pHIRP56. This deletes most of the *ybtE* gene (Fig. 1). Construction of the pCVD442 derivative pCHIRP56.2 (Table 1) required the simultaneous ligation of three fragments, the ~3.8-kb *Sph*I/*Sal*I insert from pHIRP56, a 1.34-kb *Sal*I/*Eco*RV fragment of pPSN4 (20), and pCVD442 digested with *Sph*I/*Sma*I.

Introduction of these mutant *ybt* constructs into *Y. pestis* KIM6+ was accomplished by allelic exchange (16, 20). Briefly, insertion and deletion derivatives in suicide vectors pCSIRP498.9, pCIRP1, and pCHIRP56.2 were introduced separately into KIM6+ and KIM6-2053.1+ by electroporation. For the selection of the *Y. pestis irp2* and *ybtE* deletion mutants, electroporated cells were screened for ampicillin resistance on TBA supplemented with ampicillin (50 μg/ml) for the selection of merodiploid strains. Antibiotic-resistant colonies were selected, and their plasmid profiles were examined to ensure chromosomal integration of the suicide vector derivatives. After overnight incubation in heart infusion broth (without antibiotics) at 37°C, aliquots of cointegrant strains equivalent to an optical density at 620 nm (OD_{620}) of 0.001 were plated onto CR plates containing 5% (wt/vol) sucrose. DNA fragments containing only the deleted sequences used in the construction of the *irp2* and *ybtE* mutants were used as probes in colony hybridizations of sucrose-resistant colonies. Genomic DNA was isolated from sucrose-resistant candidates as previously described (22) and used in Southern blot analyses to verify successful exchange of the mutant allele (56). These methods were used to select *Y. pestis* KIM6-2046.3 containing the in-frame *irp2* (Δ*irp2-2046.3*) deletion and KIM6-2056.1 harboring the *ybtE* (Δ*ybtE2056.1*) deletion. Final selection of strain KIM6-2054.1 (*irp1*::*kan2054.1*) was accomplished similarly but with kanamycin resistance as an additional selection.

Construction of a *Y. pestis* Psa mutant. For biosafety considerations, we constructed *Y. pestis* KIM6-2053.1+ (Δ*psa2053.1*), which is missing chromosomal genes *psaE*, *psaF*, *psaA*, *psaB*, and part of *psaC* that are required for expression of the pH 6 antigen (Psa) (37 [GenBank accession number X97759]). The deleted *psa* region in suicide plasmid pCVDPSA1 was introduced into the chromosome by allelic exchange (16, 20). Loss of this part of the *psa* locus was confirmed by Southern blot analysis (56). The absence of Psa expression was verified immunologically by colony blot assay (29) using rabbit polyclonal antiserum specific for Psa (36). Loss of Psa production results in a slight attenuation of the intravenous LD_{50} of *Y. pestis* KIM5 (Lcr^+ Pgm^-) in mice (36).

Recombinant DNA methodology. Plasmids were introduced into *E. coli* strains by standard $CaCl_2$ transformation (51). Plasmid DNAs were isolated either by alkaline lysis (3) or by precipitation with polyethylene glycol (31). Transformation of *Y. pestis* strains was performed by electroporation and has been described previously (20). Experiments requiring the use of commercially available restriction endonucleases and DNA-modifying enzymes were carried out according to the manufacturers' recommendations. Labeling of DNA fragments for use in Southern blot hybridizations was achieved by random priming using [^{32}P]dCTP (New England Nuclear) and a Rediprime labeling kit (Amersham Corp.) according to the vendors' instructions.

DNA sequencing was performed by using Sequenase version 2.0 (U.S. Biochemical Corp.) to incorporate [^{35}S]dATP (Amersham Corp.) in the presence of chain-terminating dideoxynucleotide triphosphates (52). Sequencing artifacts and compressions were resolved by using the deoxynucleotide analog 7-deaza-dGTP (Boehringer Mannheim Biochemical Corp.) and by the inclusion of dimethyl sulfoxide (Sigma Chemical Corp.) to 10% in primer-template annealing reactions. Sequencing reactions were resolved on 6% polyacrylamide gels containing 8.3 M urea (Sigma) and cast in Tris-borate-EDTA buffer (51). Dried gels were exposed to Kodak BioMax MR film at room temperature. Oligonucleotide sequencing primers were purchased (Integrated DNA Technologies, Inc.) to extend the sequence of the *ybtT* and *ybtE* open reading frames (ORFs). Homology searches of DNA and protein databases were performed by using BLAST (1). Analysis and manipulation of DNA sequence data were performed by using the Intelligenetics software suite. Sequence alignments were done with the use of the programs Pileup and Gap of the Genetics Computer Group software package version 8.1-Open VMS from the University of Wisconsin.

Protein analyses. Whole cells of *Y. pestis* strains subjected to iron-deficient or iron-sufficient growth conditions were incubated for 1 h with ^{35}S-labeled amino acids (DuPont NEN Research Products) as previously reported (21). Strains grown under iron-deficient conditions and transferred to media containing filtered culture supernatants were incubated 1.5 h at 37°C prior to the addition of ^{35}S-labeled amino acids (20). Labeled proteins were resolved by sodium dodecyl sulfate-polyacrylamide gel electrophoresis (SDS-PAGE). Equal amounts of trichloroacetic acid-precipitable counts were loaded in each lane. Dried gels were exposed to Kodak BioMax MR film at room temperature.

Cross-feeding experiments. *Y. pestis* KIM6+ and the pesticin receptor mutant KIM6-2045.1 (Δ*psn2045.1* [Table 1]) were grown at 37°C under iron-deficient conditions, and their culture supernatants were collected and filtered as previously described (20). For growth responses of the *Y. pestis ybt*, *irp*, and *psn* mutants to culture supernatants, PMH-S plates were overlayed with 0.04 OD_{620} units of cells grown in deferrated PMH and approximately 25 μl of filtered supernatants was added to wells in the plates. The plates were incubated at 37°C (Table 2). The *ybt* and *irp* mutants were tested for the ability to promote the growth of KIM6-2046.1 (*irp2*::*kan2046.1*) at 37°C by streaking the mutants adjacent to KIM6-2046.1 on PMH-S plates. Prior to streaking, the mutants were adapted to iron-deficient growth conditions in PMH at 37°C as previously described (20). Protein synthesis responses of *ybt* and *irp* mutants cultured with supernatant from KIM6-2045.1 (Δ*psn2045.1*) were determined by transferring cells acclimated to iron-deficient growth to cultures containing 50% fresh deferrated PMH and 50% filtered supernatant. Proteins were analyzed by SDS-PAGE as described above.

Virulence testing in mice. *Y. pestis* KIM5-2045.2 (Δ*psn2045.1*), KIM5-2046.4 (Δ*irp2-2046.3*), and KIM5-2053.11+ (Δ*psa2053.1*) (Table 1) were grown at 26°C in PMH containing hemin (50 μM) and kanamycin (50 μg/ml). Exponentially growing cells were harvested by centrifugation, washed, and resuspended in mouse isotonic phosphate-saline buffer (MiPBS; 149 mM NaCl, 16 mM Na_2HPO_4, 4 mM NaH_2PO_4). Female 5- to 7-week-old NIH/Swiss Webster mice (Harlan Sprague Dawley, Inc.) were injected subcutaneously with 0.1 ml of 10-fold serially diluted bacterial suspensions. Five mice were used for each bacterial dose. The actual CFU per dose was determined by serially diluting each dose in MiPBS and plating in duplicate onto TBA-kanamycin. Plates were scored following a 48-h incubation at 30°C. The mice were monitored daily for a period of 21 days. LD_{50}s were calculated by the method of Reed and Muench (49).

Nucleotide sequence accession numbers. The sequences of *ybtT* and *ybtE* have been deposited in GenBank and assigned accession number U50364. Approximately 700 nucleotides of sequence from the putative coding region of *Y. pestis irp1* have also been deposited in the GenBank database (accession number U73144). Partial sequence of the *Y. pestis irp2* gene (GenBank accession number U19396) sharing near identity with the *irp2* gene of *Y. enterocolitica* (26) has been described previously (20).

RESULTS

Sequencing and analysis of genes *ybtT* and *ybtE*. The genetic organization of the Ybt biosynthetic region which includes *ybtA*, *psn*, *irp2*, and *ybtE*, as well as *irp1* and *ybtT* (which are likely also necessary for Ybt biosynthesis), is illustrated in Fig. 1. Characterization of the Ybt region was initiated by sequencing upstream of *psn*. This identified two ORFs proximal to the *psn* gene promoter (20), which established the 3′ end of the putative *ybt* operon. The ORFs represented by these two genes, *ybtT* and *ybtE*, are predicted to encode polypeptides 267 (YbtT) and 525 (YbtE) amino acids in length with molecular masses of approximately 30 and 56 kDa, respectively. The region of DNA sequence which delineates the 3′ end of *ybtT*

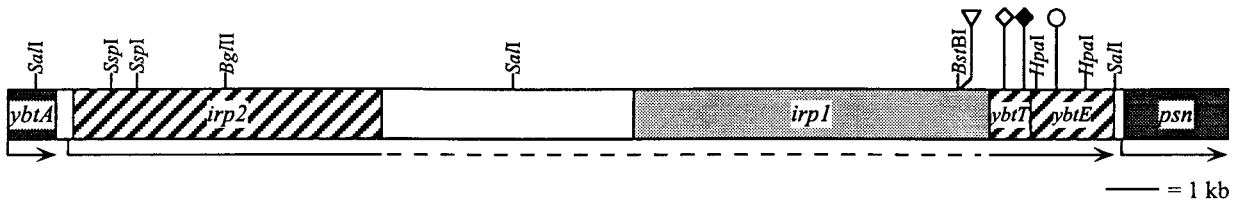

FIG. 1. Genetic organization of the Ybt biosynthetic region including the cognate yersiniabactin receptor gene (*psn*) and the AraC-type regulator, *ybtA*. Restriction sites used in generating *Y. pestis* mutant strains KIM6-2046.3 (Δ*irp2-2046.3*), KIM6-2054.1 (*irp1*::*kan2054.1*), and KIM6-2056.1 (Δ*ybtE2056.1*) are indicated. ▽ in *irp1* denotes the position of a substrate amino acid binding motif described by Schlumbohm et al. (53); ◇ and ◆ in the putative thioesterase gene, *ybtT*, represent the serine and histidine active-site motifs, respectively; a potential AMP-binding domain (○) is depicted in *ybtE*. The direction of transcription is shown by arrows. The putative polycistronic transcript spanning the Ybt biosynthetic genes is represented by the dashed arrow. In determining the domains of the ~22-kb Ybt biosynthetic region of *Y. pestis*, we used nucleotide sequence data to identify the *irp2* promoter region and the upstream ORF, *ybtA*, as well as a potential transcriptional terminator downstream of *ybtE* (19, 20).

and the 5′ end of *ybtE* is only three nucleotides in length, which suggests that the two genes are cotranscribed. Moreover, the putative start of the *ybtT* coding region appears to overlap the termination codon of an upstream ORF which we speculate is the *irp1* gene (see below). Homology searches of the DNA and protein databases by using the BLAST search engine (1) produced some significant matches. YbtT shows 59% similarity and 39% identity with a thioesterase-like protein located in the anguibactin biosynthetic gene cluster of *V. anguillarum* (18). Similarly, the *ybtE* gene product shows 61% similarity and 42% amino acid sequence identity with EntE, the 2,3-dihydroxybenzoic acid-activating enzyme utilized in the enterobactin biosynthetic pathway of *E. coli* (57). As shown in Fig. 2 and 3, both of the predicted protein sequences harbor identifiable motifs characteristic of their putative functions.

YbtT contains a consensus active-site serine motif (GXSXG) at amino acid positions 92 to 96 and a His motif (GXH) near the carboxy-terminal end of the protein (Fig. 2). The active-site serine residue and the downstream histidine, both of which are required for enzymatic activity in proven thioesterases, are separated by 135 amino acids, which falls within the range of 133 to 170 residues separating the two motifs in avian and mammalian thioesterases (12). YbtE also contains a conserved motif that is consistent with its putative role in yersiniabactin biosynthesis. A potential AMP-binding domain is located at amino acid positions 174 to 185 (Fig. 3). The presence

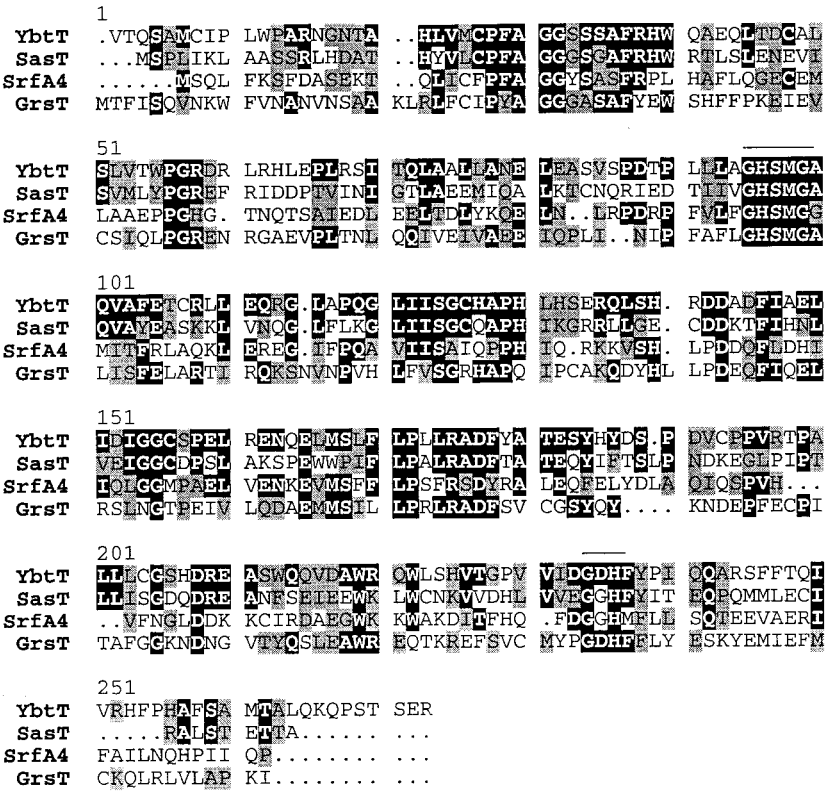

FIG. 2. Amino acid sequence alignment of prokaryotic thioesterase-like proteins. YbtT, putative thioesterase involved in *Y. pestis* yersiniabactin biosynthesis; SasT, associated with the anguibactin biosynthetic region in *V. anguillarum* (18); SrfA4, a thioesterase-like protein involved in surfactin biosynthesis from *B. subtilis* (13); and GrsT, first gene product in the gramicidin S biosynthetic operon from *Bacillus brevis* (34). Residues with identity with YbtT are in white with a solid black background. Conservative amino acid substitutions are shaded. The active-site serine and histidine motifs are overlined.

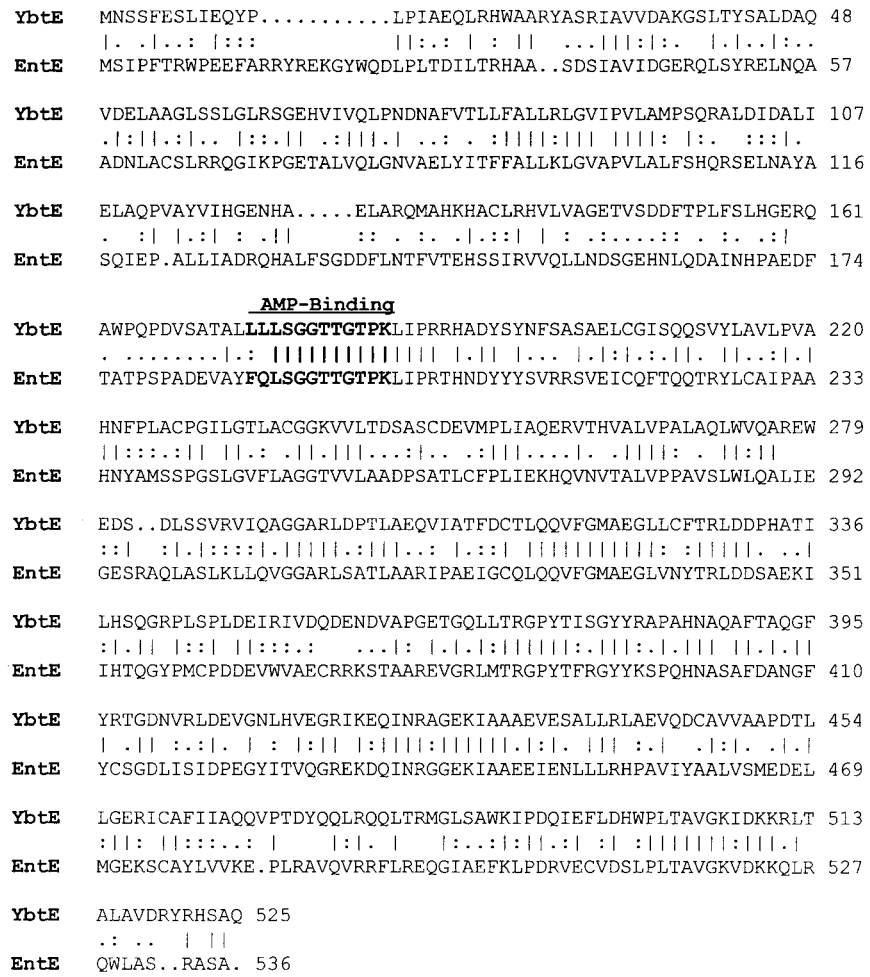

FIG. 3. Amino acid sequence alignment of *Y. pestis* YbtE and *E. coli* EntE, the 2,3-dihydroxybenzoic acid-activating enzyme necessary for enterobactin biosynthesis. The putative AMP-binding domains are in boldface. Identities are indicated by vertical lines, conservative substitutions are denoted by colons, and semiconservative amino acid changes are represented by periods.

of this domain in *E. coli* EntE underscores its putative function as an AMP ligase (57).

Pleiotropic effects of the *ybtE* mutant in *Y. pestis* KIM6+. To determine the effect of a YbtE$^-$ mutant on the expression of other *ybt* and *irp*-encoded proteins, a 984-bp *Hpa*I fragment was excised from *ybtE* (Fig. 1). Cells carrying this mutation (Δ*ybtE2056.1*) were unable to grow on PMH-S (20) at 37°C (Table 2). In a previous study, an *irp2*::*kan2046.1* strain of *Y. pestis* (KIM6-2046.1) was unable to grow on PMH-S plates at 37°C and displayed a Ybt$^-$ Psn$^-$ phenotype. However, KIM6-2046.1 could be fed by culture supernatants of Ybt-producing strains which promoted its growth at 37°C on PMH-S plates and restored Psn expression (20). We have conducted similar feeding experiments with *Y. pestis* KIM6-2056.1 (Δ*ybtE2056.1*). KIM6-2056.1 was defective in Ybt production, as demonstrated by its inability to stimulate growth of the

TABLE 2. Growth of *Y. pestis* KIM6+ and its *ybt irp* mutant derivatives on PMH-S

Strain	37°C growth on PMH-S[a]	Cross-feeding of KIM6-2046.1 (*irp2*::*kan2046.1*) by[b]	Cross-fed by KIM6+ or KIM6-2045.1 (Δ*psn2045.1*)[c]
KIM6+ (Psn$^+$ Ybt$^+$)	+	+	ND[d]
KIM6-2045.1 (Δ*psn2045.1*)	−	+	−
KIM6-2046.1 (*irp2*::*kan2046.1*)	−	−	+
KIM6-2046.3 (Δ*irp2-2046.3*)	−	−	+
KIM6-2046.3(pIRP2) (Δ*irp2-2046.3*/*irp2*$^+$)	+	+	ND
KIM6-2054.1 (*irp1*::*kan2054.1*)	−	−	+
KIM6-2056.1 (Δ*ybtE2056.1*)	−	−	+

[a] The presence or absence of growth on PMH-S plates at 37°C is denoted as a + or −, respectively.
[b] Each strain was tested for its ability to promote the growth of KIM6-2046.1 (*irp2*::*kan2046.1*) at 37°C by streaking adjacent to KIM6-2046.1 on PMH-S.
[c] Each strain was tested for its ability to be cross-fed by the Ybt$^+$ spent culture supernatants of either KIM6+ or KIM6-2045.1 (Δ*psn2045.1*) at 37°C on PMH-S.
[d] ND, not done.

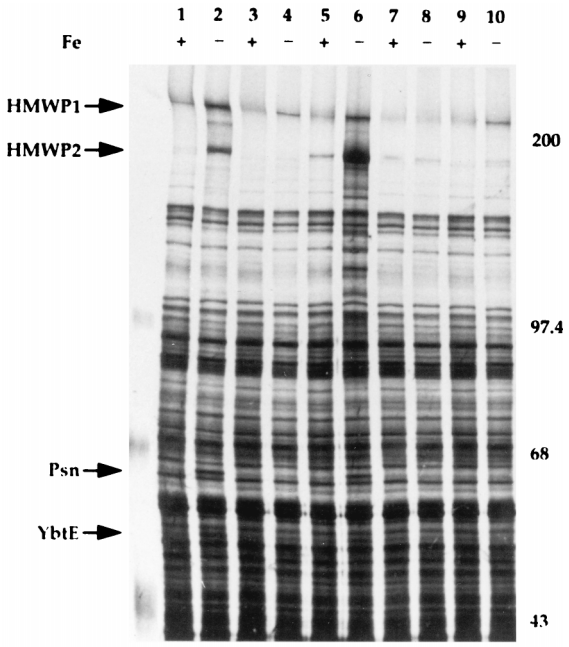

FIG. 4. Whole-cell proteins from *Y. pestis* strains grown in PMH in the presence (+) or absence (−) of 10 μM $FeCl_3$ (Fe). Cultures from *Y. pestis* KIM6+ (lanes 1 and 2), KIM6-2046.3 (Δ*irp2-2046.3*, lanes 3 and 4), KIM6-2046.3 containing the HMWP2-expressing plasmid pIRP2 (lanes 5 and 6), KIM6-2054.1 (*irp1*::*kan2054.1*, lanes 7 and 8), and KIM6-2056.1 (Δ*ybtE2056.1*, lanes 9 and 10) were incubated with ^{35}S-labeled amino acids, and total cellular proteins were resolved by SDS-PAGE. The molecular masses of the protein standards are indicated in kilodaltons on the right. Arrows point to the iron-regulated proteins HMWP1 (240 kDa), HMWP2 (190 kDa), Psn (68 kDa), and YbtE (56 kDa). Although the relative migration of HMWP2 in pathogenic *Yersinia* is estimated at 190 kDa (8), sequence analysis of the *irp2* gene from *Y. enterocolitica* has established the predicted molecular mass to be 228 kDa (26).

irp2::*kan2046.1* strain, KIM6-2046.1. However, the Δ*ybtE* mutant strain was readily cross-fed by the Δ*psn2045.1* mutant, KIM6-2045.1 (Table 2). The effects of the *ybtE* deletion on other iron-regulated proteins were determined by incubating KIM6-2056.1 (Δ*ybtE2056.1*) cells for 1 h with ^{35}S-labeled amino acids after the cells had become acclimated to growth in the defined, iron-deficient medium PMH (58). SDS-PAGE analysis indicated that despite *ybtE*'s position as the final coding region in the putative *ybt* operon, loss of the *ybtE* gene product significantly inhibited the expression of HMWP1 and HMWP2 and obviated the iron-regulated expression of the *psn* gene product (Fig. 4, lane 10).

Mapping and mutagenesis of the *irp1* gene of *Y. pestis*. To determine the position of *irp1* in the *ybt* operon of *Y. pestis*, we constructed a mutant (KIM6-2054.1) by insertion of a *kan* cassette into the *Bst*BI site shown in Fig. 1. Strain KIM6-2054.1 was Ybt$^-$, being unable to grow on PMH-S plates at 37°C. This growth defect was restored by cross-feeding with a culture supernatant containing Ybt (Table 2). SDS-PAGE analysis of the polypeptide profile of KIM6-2054.1 (*irp1*::*kan2054.1*) showed that in addition to the anticipated loss of HMWP1 expression, YbtE and Psn were not expressed and the synthesis of HMWP2 was significantly reduced (Fig. 4, lane 8).

The DNA sequence of the area spanning the *Bst*BI insertion site was determined in order to identify the disrupted gene. Examination of the predicted ORFs in this region revealed a motif with strong homology to the consensus sequence, F(F,Y)XLGG(H,D)S(L,I). This sequence has been characterized as the site for covalent substrate amino acid binding (SBS) and is found at the carboxy-terminal ends of the activation domains prevalent in enzymes involved in the biosynthesis of the peptide antibiotics gramicidin S and tyrocidin (53) and the lipopeptide detergent surfactin (13). Most notably, however, the motif is also present in the HMWP2 protein of *Y. enterocolitica*, with related sequences evident in the siderophore biosynthetic polypeptides AngR and EntF expressed in *V. anguillarum* and *E. coli*, respectively (26) (Fig. 5). Multiple sequence alignment of the SBS domains was performed by using the program Pileup (University of Wisconsin Genetics Computer Group software package, version 8.1-OpenVMS). The serine residue present at position 8 of the consensus motif acts as the substrate binding residue for either 4′-phosphopantetheine or an activated amino acid. 4′-Phosphopantetheine serves as a cofactor bearing a sulfhydryl group involved in thioester bond formation with amino acid substrates and in peptidyl transfer (53). Based on the relative positions within these nonribosomal peptide bond-forming enzymes to which the *Y. pestis* SBS motif has homology, we have estimated that the *irp1* gene product terminates adjacent to the start of YbtT, a thioesterase-like protein involved in *S*-acyl fatty acid synthesis, and begins some 5 to 6 kb downstream of the *irp2* termination codon as illustrated in Fig. 1. However, we cannot exclude the possibility that a separate ORF is positioned between *irp1* and *ybtT*.

Analysis of the *Y. pestis irp2* in-frame deletion mutant. Previously, insertion of a *kan* cassette into the *irp2* gene resulted in a loss of expression of both HMWPs as well as the 56-kDa protein, YbtE, and Psn (20). The lack of expression of HMWP1 and other polypeptides related to Ybt biosynthesis in these experiments was due ostensibly to the polar effects of the *irp2* mutation (7, 20). To control for polarity effects on downstream genes, we have constructed an *irp2* in-frame deletion mutant by excising a 471-bp *Ssp*I fragment near the amino-terminal end of the HMWP2 coding region as depicted in Fig. 1. The *Ssp*I sites were determined from the DNA sequence of the *Y. enterocolitica irp2* gene (26) and are conserved in *Y. pestis*. The mutant, designated KIM6-2046.3, encodes an *irp2* gene product truncated by 157 amino acids. SDS-PAGE analysis of ^{35}S-labeled whole-cell lysates of the *irp2* mutant grown in PMH revealed that iron-regulated HMWP1 expression is maintained in KIM6-2046.3 (Fig. 4, lanes 3 and 4), but at levels that are markedly lower than those for wild-type KIM6+ (Fig. 4, lane 2). Moreover, under conditions of iron-deficient growth, the expression of YbtE and Psn was undetectable in KIM6-2046.3, and a putative truncated *irp2* gene product, although visible by autoradiography, was present only in trace amounts (Fig. 4, lane 4). *Y. pestis* KIM6-2046.3 was unable to grow at 37°C on the iron-deficient medium PMH-S, indicating a defect in Ybt biosynthesis. Growth was restored by cross-feeding with the culture supernatant of a Ybt-producing strain (Table 2). Complementation of the *irp2* deletion mutant with the HMWP2-expressing plasmid pIRP2 (20) restored synthesis of HMWP1, YbtE, and Psn to wild-type levels and resulted in overexpression of HMWP2 (Fig. 4, lane 6) in cells grown in the absence of iron. Strain KIM6-2046.3 (pIRP2) was able to grow at 37°C on PMH-S and demonstrated the ability to cross-feed the Ybt$^-$ mutant KIM6-2046.1 (*irp2*::*kan2046.1* [Table 2]).

Cross-feeding of *ybt* mutant strains. The results shown in Table 2 summarize the growth characteristics of *Y. pestis* mutants KIM6-2046.3 (Δ*irp2-2046.3*), KIM6-2054.1 (*irp1*::*kan2054.1*), and KIM6-2056.1 (Δ*ybtE2056.1*) on PMH-S at 37°C and demonstrate the ability of these strains to be cross-fed by culture supernatant from KIM6-2045.1 (Δ*psn2045.1*). Culture supernatant from KIM6-2045.1 not only promoted growth of these mutants on PMH-S plates at 37°C but restored expression of Psn and the *ybt*- and *irp*-encoded proteins,

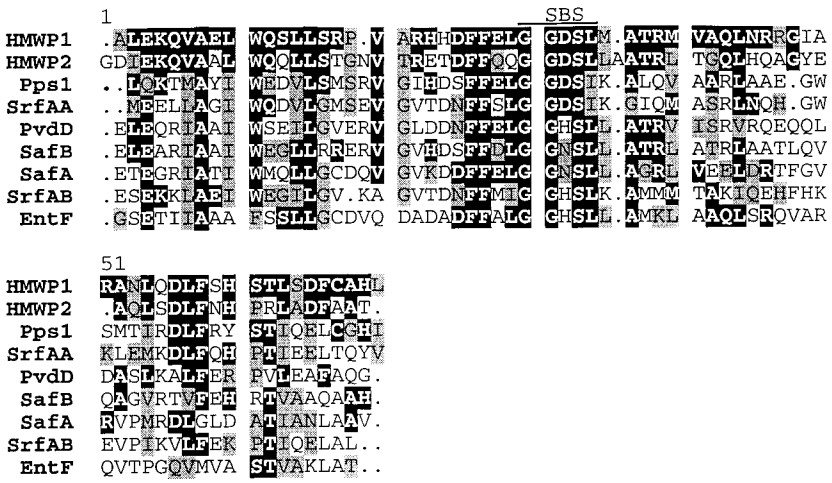

FIG. 5. Alignment of the predicted amino acid sequence within the putative *irp1* coding region of *Y. pestis* to the covalent SBS regions of polypeptides involved in the biosynthesis of peptide antibiotics and siderophores. HMWP2 (2,035 residues), amino acids 1407 to 1473 of the *irp2* gene product from *Y. enterocolitica* involved in yersiniabactin biosynthesis (26); Pps1 (2,561 residues), amino acids 2012 to 2077 of peptide synthetase ORF1 of *B. subtilis* (63); SrfAA (3,589 residues), amino acids 3043 to 3108 of SrfA ORF1 of the *B. subtilis* surfactin synthetase biosynthetic region (13); PvdD (2,449 residues), amino acids 1023 to 1089 of pyoverdine synthetase D from *P. aeruginosa* (39); SafB (1,770 residues), amino acids 1679 to 1745 of saframycin Mx1 synthetase B from *Myxococcus xanthus*; SafA (2,605 residues), amino acids 998 to 1064 of saframycin Mx1 synthetase A from *M. xanthus* (47); SrfAB (3,588 residues), amino acids 969 to 1034 of SrfA ORF2 of the *B. subtilis* surfactin synthetase biosynthetic region (13); EntF (1,294 residues), amino acids 975 to 1040 of the *E. coli entF* gene product involved in enterobactin biosynthesis (50). The domains for each of the proteins shown represent the regions of strongest sequence similarity. Other regions of homology within these ORFs include SrfAA (amino acids 975 to 1040 and 2015 to 2080), SrfAB (amino acids 2010 to 2075 and 3035 to 3100), SafA (amino acids 2113 to 2179), and PvdD (amino acids 2084 to 2150). Highlighting of identities and conservative substitutions, as described in the legend to Fig. 2, is relative to HMWP1.

HMWP1, HMWP2, and YbtE, to wild-type levels (Fig. 6). We determined this by radiolabeling cells from each of the *Y. pestis* mutant strains in the presence or absence of spent supernatant from KIM6-2045.1 under iron-deficient conditions as described in Materials and Methods. SDS-PAGE analysis of the ^{35}S-labeled proteins revealed that the expression of HMWP2 and Psn was restored to levels that were indistinguishable from those of the wild-type strain, KIM6+, in the *irp1*::*kan* mutant KIM6-2054.1 grown in the presence of the Ybt-containing supernatant (Fig. 6, lane 2). Loss of *psn* gene expression as well as the loss or significant reduction in the expression of HMWP1, the putative truncated HMWP2, and YbtE was evident in *Y. pestis* KIM6-2046.3 (Δ*irp2-2046.3*) (Fig. 6, lane 3). Again, expression of all of these proteins was restored (Fig. 6, lane 4) in the presence of the growth-promoting supernatant from KIM6-2045.1 (Δ*psn2045.1*). Similar results can also be seen for the mutant KIM6-2056.1 (Δ*ybtE2056.1*), in which the absence of detectable levels of HMWP1, HMWP2, and Psn is abrogated in the presence of culture supernatant from KIM6-2045.1 (Δ*psn2045.1*) (Fig. 6, lanes 5 and 6, respectively).

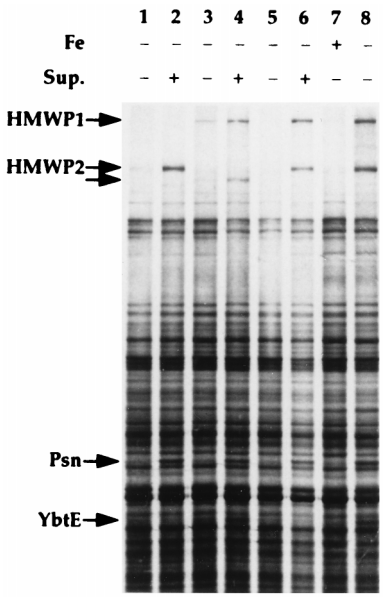

FIG. 6. Whole-cell proteins of *Y. pestis* strains grown in PMH in the presence (+) or absence (−) of 10 μM $FeCl_3$ (Fe) and spent culture supernatants (Sup.) from *Y. pestis* KIM6-2045.1 (Δ*psn2045.1*). Cultures from KIM6-2054.1 (*irp1*::*kan2054.1*; lanes 1 and 2), KIM6-2046.3 (Δ*irp2-2046.3*; lanes 3 and 4), KIM6-2056.1 (Δ*ybtE2056.1*; lanes 5 and 6), and KIM6+ (lanes 7 and 8) were incubated with ^{35}S-labeled amino acids, and total cellular proteins were resolved by SDS-PAGE. Arrows point to the iron-regulated proteins HMWP1 (240 kDa), HMWP2 (190 kDa), Psn (68 kDa), and YbtE (56 kDa). The unlabeled arrow points to the putative, truncated *irp2* gene product (lane 4) expressed by the *Y. pestis* in-frame deletion mutant KIM6-2046.3 (Δ*irp2-2046.3*).

These results clearly demonstrate that Ybt is involved in facilitating the iron-regulated expression of its cognate receptor and in activating transcription of the *ybt* biosynthetic genes. The nature of Ybt-mediated gene activation is unclear but may involve the interaction of Ybt with the AraC-type regulator, YbtA (19).

Infection of mice. To determine the importance of *psn* and *irp2* gene expression in the pathogenesis of *Y. pestis* in the mouse, we compared the LD_{50}s of the *psn* and *irp2* deletion strains, KIM5-2045.21 (Δ*psn2045.1* Δ*psa2053.1 yopJ*::Mu*d*I1734) and KIM5-2046.41 (Δ*irp2-2046.3* Δ*psa2053.1 yopJ*::Mu*d*I1734), respectively, to that of the slightly attenuated *Y. pestis* parent strain KIM5-2053.11+ (Δ*psa2053.1 yopJ*::Mu*d*I1734 [Table 1]) as described in Materials and Methods. Groups of five NIH/Swiss Webster mice were infected subcutaneously with bacterial dosages starting at ~10 CFU and increasing in 10-fold increments to 10^4 CFU for strain KIM5-2053.11+ and ranging from 10 to 10^6 CFU for strains KIM5-2045.21 and KIM5-2046.41. An LD_{50} of 1.3×10^2 CFU determined for the parent strain KIM5-2053.11+ was significantly lower than values of

$>2.9 \times 10^5$ and $>1.3 \times 10^6$ CFU calculated for the *Y. pestis* mutants KIM5-2045.2 and KIM5-2046.4, respectively.

DISCUSSION

The determination of siderophore production in the plague bacillus, *Y. pestis*, has not evolved without some controversy. Early studies suggested that some cells within a *Y. pestis* population were siderophore producers, but this was not corroborated by standard siderophore detection methods (45, 65). Only recently have cross-feeding studies and mutant analyses independently confirmed the original observation of siderophore production in *Y. pestis* (20, 65). While the *Y. pestis* siderophore has not yet been isolated, clues regarding its structure may be gleaned from recent data describing the isolation and extensive elemental analyses of the *Y. enterocolitica* siderophore, Ybt (10, 17, 27). The structure of Ybt is closely related to those of the siderophores pyochelin and anguibactin produced by *P. aeruginosa* and *V. anguillarum*, respectively (10, 17). The biosynthetic genes for Ybt have not been conclusively demonstrated in *Y. enterocolitica*; however, production of this iron-chelating compound has been shown to strongly correlate with the expression of polypeptides HMWP1 and HMWP2 (11). The 228-kDa HMWP2 exhibits extensive homology to a family of adenylate-forming enzymes involved in the nonribosomal formation of peptide bonds whose activities include the biosynthesis of siderophores and peptide antibiotics (26). Moreover, HMWP1 and HMWP2 are expressed only in pathogenic strains of *Yersinia* and are correlated with virulence (8, 9).

We have identified an ~22-kb region of the *pgm* locus in *Y. pestis* KIM6+ immediately adjacent to the *psn* gene (20, 21) which includes the *irp1* and *irp2* genes encoding polypeptides HMWP1 and HMWP2, respectively, as well as three previously undescribed ORFs. These have been designated *ybtA*, *ybtT*, and *ybtE* and are predicted to encode, respectively, an AraC-type transcriptional activator (19), a thioesterase-like protein (18), and a 56-kDa protein with similarity to the dihydroxybenzoic acid-activating enzyme, EntE, necessary for enterobactin biosynthesis in *E. coli* (57). This region of the *pgm* locus in conjunction with the downstream pesticin receptor gene represents the *ybt-psn* gene cluster and is responsible for the biosynthesis of Ybt and its cognate receptor. It was shown previously that a 41-kb region of the *pgm* locus which included the *ybt-psn* operons was able to restore pesticin sensitivity and the iron-regulated expression of proteins with sizes of 240, 190, 68, and 56 kDa to Pgm^- strains of *Y. pestis* (20, 21). A more detailed perspective of the Ybt biosynthetic region is shown in Fig. 1. Nucleotide sequencing data and mutational analysis indicate that the locus is delimited at its 5′ end by the *irp2* promoter region (19) and at its distal extreme by a putative transcriptional terminator and the *psn* promoter region following *ybtE* (20). The data presented suggest that *irp2*, *irp1*, *ybtT*, and *ybtE* form a polycistronic operon producing a transcript ~20.4 kb in length. Evidence for this is supported by the lack of intergenic space between *ybtE* and *ybtT* and between *ybtT* and the putative *irp1* ORF located immediately upstream. Moreover, the mutations *irp2*::*kan2046.1* (20) and *irp1*::*kan2054.1* are polar and abrogate expression of downstream Ybt biosynthetic genes. *Y. pestis* strains carrying these mutations also exhibit an absence of *psn* gene expression. This loss of expression of downstream *irp1* and/or *ybtE* sequences is not reversed by the addition of supernatant from Ybt-producing strains; however, Psn production is restored indicating that the polar effects resulting from the *kan* cassette insertions extend into but not beyond *ybtE*. These and earlier observations (7, 19, 20) support the *ybt* operon model and suggest that despite the loss of Psn in the polar mutants, the *psn* gene is transcribed separately and that optimal *psn* expression is Ybt dependent (see below).

Strong sequence identity with the *irp2* gene of *Y. enterocolitica* and data presented here favor the involvement of the *Y. pestis irp2* gene in Ybt biosynthesis (20, 26). We were able to complement an *irp2* in-frame deletion mutant, KIM6-2046.3(Δ*irp2-2046.3*), with a recombinant plasmid (pIRP2) expressing the HMWP2 protein. KIM6-2046.3 (pIRP2) grew on PMH-S plates at 37°C and was able to cross-feed the Ybt^- mutant KIM6-2046.1 (*irp2*::*kan2046.1*). SDS-PAGE analysis of ^{35}S-labeled cell extracts of KIM6-2046.3(pIRP2) revealed that expression of HMWP1, HMWP2, YbtE, and Psn was restored (Fig. 4, lane 6). Mutational analysis of the *Y. pestis ybtE* gene indicates that its role in Ybt biosynthesis is also essential.

An ORF immediately upstream of the YbtE coding region encodes a protein similar to a thioesterase-like protein which has been linked to the plasmid-encoded anguibactin siderophore biosynthetic region of *V. anguillarum* (18). Although the 30-kDa gene product, designated YbtT, has not been detected by SDS-PAGE, DNA sequence analysis suggests that it is translationally coupled to YbtE. As shown in Fig. 2 and 3, both of the predicted protein sequences for YbtT and YbtE harbor identifiable motifs, which in the absence of data from enzymatic assays allow for a degree of plausibility regarding the putative function of these polypeptides and their role in Ybt biosynthesis. Preliminary sequence analysis and characterization of an insertion mutant have enabled us to tentatively map the *irp1* gene upstream and probably adjacent to *ybtT*. This is based on the loss of HMWP1 expression in strain KIM6-2054.1 (*irp1*::*kan2054.1*), which was not restored in supernatant cross-feeding experiments (Fig. 6, lane 2), and on preliminary sequence data indicating the presence of a consensus SBS motif common to peptide antibiotic synthetases (53). This supports the observation by Guilvout et al. (26) that HMWP1 and HMWP2 may form part of a multienzyme complex mediating the nonribosomal synthesis of a peptide or peptide-like structure. Although not conclusive, these data predict a role for HMWP1 in the biosynthesis of yersiniabactin. Since the sequence homologies to HMWP1 occur mainly in the carboxy-terminal regions of their respective biosynthetic enzymes, it is reasonable to speculate that *irp1* is contiguous with *ybtT*, but this does not preclude the possibility of an unidentified ORF between *irp1* and *ybtT*. The *irp2* and *irp1* genes of *Y. pestis*, nevertheless, are not contiguous, and no data are presently available concerning the ~6-kb intervening segment.

We have shown that an insertional mutation in *irp1* as well as deletions constructed within *irp2* and *ybtE* abrogate Ybt production under iron-deficient conditions and prevent growth of these strains at 37°C on stringently deferrated media. Additionally, we observed a significant decrease in the expression of the *psn* gene product in *ybtE*, *irp1*, and *irp2* mutants grown in the absence of iron. This phenotype was readily reversible by the addition of spent culture supernatants from Ybt^+ strains of *Y. pestis*, which restored Psn production to wild-type levels. Moreover, there was diminished expression of *irp*- and *ybt*-encoded proteins in the Δ*irp2* mutant, KIM6-2046.3 (Δ*irp2-2046.3*), under conditions of iron-deficient growth. Incubation with Ybt-containing culture supernatant restored expression of the *irp1*, truncated *irp2′*, and *ybtE* gene products as well as Psn in KIM6-2046.3 (Fig. 6, lanes 3 and 4). These observations suggest that in addition to regulation by Fur (20, 59), maximal expression of Psn, HMWP1, HMWP2, YbtE, and presumably YbtT may depend on the iron-regulated synthesis of Ybt and indicate that Ybt serves as an essential cofactor in promoting

optimal expression of the genes required for its own biosynthesis. The siderophore-specific induction of iron transport receptors has also been reported in *P. aeruginosa* (23). In *E. coli*, the ferric dicitrate uptake system requires citrate to initiate a signal transduction cascade that results in the activation of an alternative sigma factor which directs transcription of *fec* transport genes (42). However, in addition to Ybt itself, an AraC-type regulator, YbtA, is also essential for the activation of expression of the Ybt receptor and biosynthetic genes (19). We have identified *ybtA* as the ORF upstream of *irp2* having strong similarity to that for PchR (19), a transcriptional activator of pyochelin biosynthesis, and to that for its cognate receptor, FptA (28). Construction of a *ybtA* mutant results in a Ybt^- Psn^- phenotype which is not restored to wild type by the addition of exogenous siderophore from spent culture supernatants (19).

In the decades that have followed the observation that virulence in mice can be restored to Pgm^- strains of *Y. pestis* by coadministration of supplemental iron or hemin (32), several groups have begun to define the roles of the Ybt genetic loci shared among the *Yersinia* and their contributions to virulence. Mutagenesis of the *irp2* gene of *Y. pseudotuberculosis* was shown to abrogate expression of both HMWP1 and HMWP2 and cause a decrease in virulence in the mouse model that was independent of the route of infection (7). An *fyuA* mutant of *Y. enterocolitica* and an undefined pesticin-resistant mutant of *Y. pestis* exhibited reduced virulence in mice which could be restored by complementation with the cloned *fyuA* gene and conjugal transfer of the pesticin sensitivity determinant, respectively (35, 48). Consistent with these findings, we have shown that *Y. pestis* strains deficient in Ybt production [KIM5-2046.4 (Δ*irp2-2046.3*)] or its cognate receptor, Psn [KIM5-2045.2 (Δ*psn2045.1*)], exhibit a dramatic loss of virulence in mice infected subcutaneously. The Δ*irp2* mutation caused at least a 10,000-fold loss of virulence, while a >2,200-fold loss of virulence was observed with the Δ*psn* mutation. This finding indicates that a major cause of the avirulence of Δ*pgm* strains of *Y. pestis* from peripheral routes of infection is a lack of the Ybt siderophore transport system.

ACKNOWLEDGMENTS

This work was supported by Public Health Services grant AI33481 from the National Institutes of Health.

We thank James Kaper for generously providing pCVD442 and Susan Straley for providing pDG6 and antibodies against the pH 6 antigen. We also acknowledge the technical support of Vincent Bertolino. Finally, we thank Heather Jones for constructing *Y. pestis* strain KIM6-2053+.

REFERENCES

1. **Altschul, S. F., W. Gish, W. Miller, E. W. Myers, and D. J. Lipman.** 1990. Basic local alignment search tool. J. Mol. Biol. **215:**403–410.
2. **Ausubel, F. M., R. Brent, R. E. Kingston, D. D. Moore, J. G. Seidman, J. A. Smith, and K. Struhl (ed.).** 1987. Current protocols in molecular biology. John Wiley & Sons, New York, N.Y.
3. **Birnboim, H. C., and J. Doly.** 1979. A rapid alkaline extraction procedure for screening recombinant plasmid DNA. Nucleic Acids Res. **7:**1513–1523.
4. **Braun, V., and K. Hantke.** 1991. Genetics of bacterial iron transport, p. 107–138. *In* G. Winkelmann (ed.), Handbook of microbial iron chelates. CRC Press, Inc., Boca Raton, Fla.
5. **Brubaker, R. R.** 1969. Mutation rate to nonpigmentation in *Pasteurella pestis*. J. Bacteriol. **98:**1404–1406.
6. **Brubaker, R. R.** 1991. Factors promoting acute and chronic diseases caused by yersiniae. Clin. Microbiol. Rev. **4:**309–324.
7. **Carniel, E., A. Guiyoule, I. Guilvout, and O. Mercereau-Pujalon.** 1992. Molecular cloning, iron-regulation and mutagenesis of the *irp2* gene encoding HMWP2, a protein specific for the highly pathogenic *Yersinia*. Mol. Microbiol. **6:**379–388.
8. **Carniel, E., D. Mazigh, and H. H. Mollaret.** 1987. Expression of iron-regulated proteins in *Yersinia* species and their relation to virulence. Infect. Immun. **55:**277–280.
9. **Carniel, E., O. Mercereau-Puijalon, and S. Bonnefoy.** 1989. The gene coding for the 190,000-dalton iron-regulated protein of *Yersinia* species is present only in the highly pathogenic strains. Infect. Immun. **57:**1211–1217.
10. **Chambers, C. E., D. D. McIntyre, M. Mouck, and P. A. Sokol.** 1996. Physical and structural characterization of yersiniophore, a siderophore produced by clinical isolates of *Yersinia enterocolitica*. Biometals **9:**157–167.
11. **Chambers, C. E., and P. A. Sokol.** 1994. Comparison of siderophore production and utilization in pathogenic and environmental isolates of *Yersinia enterocolitica*. J. Clin. Microbiol. **32:**32–39.
12. **Cho, H., and J. E. Cronan, Jr.** 1993. *Escherichia coli* thioesterase I, molecular cloning and sequencing of the structural gene and identification as a periplasmic enzyme. J. Biol. Chem. **268:**9238–9245.
13. **Cosmina, P., F. Rodriguez, F. de Ferra, G. Grandi, M. Perego, G. Venema, and D. van Sinderen.** 1993. Sequence and analysis of the genetic locus responsible for surfactin synthesis in *Bacillus subtilis*. Mol. Microbiol. **8:**821–831.
14. **Crichton, R. R., and M. Charloteaux-Wauters.** 1987. Iron transport and storage. Eur. J. Biochem. **164:**485–506.
15. **De Lorenzo, V., F. Giovannini, M. Herrero, and J. B. Neilands.** 1988. Metal ion regulation of gene expression. Fur repressor-operator interaction of the promoter region of the aerobactin system of pColV-K30. J. Mol. Biol. **203:**875–884.
16. **Donnenberg, M. S., and J. B. Kaper.** 1991. Construction of an *eae* deletion mutant of enteropathogenic *Escherichia coli* by using a positive-selection suicide vector. Infect. Immun. **59:**4310–4317.
17. **Drechsel, H., H. Stephan, R. Lotz, H. Haag, H. Zähner, K. Hantke, and G. Jung.** 1995. Structure elucidation of yersiniabactin, a siderophore from highly virulent *Yersinia* strains. Liebigs Ann. **1995:**1727–1733.
18. **Farrell, D. H., P. Mikesell, L. A. Actis, and J. H. Crosa.** 1990. A regulatory gene, *angR*, of the iron uptake system of *Vibrio anguillarum*: similarity with phage P22 *cro* and regulation by iron. Gene **86:**45–51.
19. **Fetherston, J. D., S. W. Bearden, and R. D. Perry.** 1996. YbtA, an AraC-type regulator of the *Yersinia pestis* pesticin/yersiniabactin receptor. Mol. Microbiol. **22:**315–325.
20. **Fetherston, J. D., J. W. Lillard, Jr., and R. D. Perry.** 1995. Analysis of the pesticin receptor from *Yersinia pestis*: role in iron-deficient growth and possible regulation by its siderophore. J. Bacteriol. **177:**1824–1833.
21. **Fetherston, J. D., and R. D. Perry.** 1994. The pigmentation locus of *Yersinia pestis* KIM6+ is flanked by an insertion sequence and includes the structural genes for pesticin sensitivity and HMWP2. Mol. Microbiol. **13:**697–708.
22. **Fetherston, J. D., P. Schuetze, and R. D. Perry.** 1992. Loss of the pigmentation phenotype in *Yersinia pestis* is due to the spontaneous deletion of 102 kb of chromosomal DNA which is flanked by a repetitive element. Mol. Microbiol. **6:**2693–2704.
23. **Gensberg, K., K. Hughes, and A. W. Smith.** 1992. Siderophore-specific induction of iron uptake in *Pseudomonas aeruginosa*. J. Gen. Microbiol. **138:**2381–2387.
24. **Griffiths, E.** 1987. Iron in biological systems, p. 1–25. *In* J. J. Bullen and E. Griffiths (ed.), Iron and infection: molecular, physiological, and clinical aspects. John Wiley & Sons, Inc., New York, N.Y.
25. **Guerinot, M. L.** 1994. Microbial iron transport. Annu. Rev. Microbiol. **48:**743–772.
26. **Guilvout, I., O. Mercereau-Pujalon, S. Bonnefey, A. P. Pugsley, and E. Carniel.** 1993. High-molecular-weight protein 2 of *Yersinia enterocolitica* is homologous to AngR of *Vibrio anguillarum* and belongs to a family of proteins involved in nonribosomal peptide synthesis. J. Bacteriol. **175:**5488–5504.
27. **Haag, H., K. Hantke, H. Drechsel, I. Stojiljkovic, G. Jung, and H. Zähner.** 1993. Purification of yersiniabactin: a siderophore and possible virulence factor of *Yersinia enterocolitica*. J. Gen. Microbiol. **139:**2159–2165.
28. **Heinrichs, D. E., and K. Poole.** 1993. Cloning and sequence analysis of a gene (*pchR*) encoding an AraC family activator of pyochelin and ferripyochelin receptor synthesis in *Pseudomonas aeruginosa*. J. Bacteriol. **175:**5882–5889.
29. **Helfman, D. M., J. R. Feramisco, J. C. Fiddes, G. P. Thomas, and S. H. Hughes.** 1983. Identification of clones that encode chicken tropomyosin by direct immunological screening of a cDNA expression library. Proc. Natl. Acad. Sci. USA **80:**31–35.
30. **Higuchi, K., and J. L. Smith.** 1961. Studies on the nutrition and physiology of *Pasteurella pestis*. VI. A differential plating medium for the estimation of the mutation rate to avirulence. J. Bacteriol. **81:**605–608.
31. **Humphreys, G. O., G. A. Willshaw, and E. S. Anderson.** 1975. A simple method for the preparation of large quantities of pure plasmid DNA. Biochim. Biophys. Acta **383:**457–463.
32. **Jackson, S., and T. W. Burrows.** 1956. The virulence-enhancing effect of iron on nonpigmented mutants of virulent strains of *Pasteurella pestis*. Br. J. Exp. Pathol. **37:**577–583.
33. **Jackson, S., and T. W. Burrows.** 1956. The pigmentation of *Pasteurella pestis* on a defined medium containing haemin. Br. J. Exp. Pathol. **37:**570–576.
34. **Krätzschmar, J., M. Krause, and M. A. Marahiel.** 1989. Gramacidin S biosynthesis operon containing the structural genes *grsA* and *grsB* has an

open reading frame encoding a protein homologous to fatty acid thioesterases. J. Bacteriol. **171:**5422–5429.
35. **Kutyrev, V. V., A. A. Filippov, O. S. Oparina, and O. A. Protsenko.** 1992. Analysis of *Yersinia pestis* chromosomal determinants Pgm^+ and Pst^s associated with virulence. Microb. Pathog. **12:**177–186.
36. **Lindler, L. E., M. S. Klempner, and S. C. Straley.** 1990. *Yersinia pestis* pH 6 antigen: genetic, biochemical, and virulence characterization of a protein involved in the pathogenesis of bubonic plague. Infect. Immun. **58:**2569–2577.
37. **Lindler, L. E., and B. D. Tall.** 1993. *Yersinia pestis* pH6 antigen forms fimbriae and is induced by intracellular association with macrophages. Mol. Microbiol. **8:**311–324.
38. **Litwin, C. M., and S. B. Calderwood.** 1993. Role of iron in regulation of virulence genes. Clin. Microbiol. Rev. **6:**137–149.
39. **Merriman, T. R., M. E. Merriman, and I. L. Lamont.** 1995. Nucleotide sequence of *pvdD*, a pyoverdine biosynthetic gene from *Pseudomonas aeruginosa*: PvdD has similarity to peptide synthetases. J. Bacteriol. **177:**252–258.
40. **Mietzner, T. A., and S. A. Morse.** 1994. The role of iron-binding proteins in the survival of pathogenic bacteria. Annu. Rev. Nutr. **14:**471–493.
41. **Miller, V. L., and J. J. Mekalanos.** 1988. A novel suicide vector and its use in construction of insertion mutations: osmoregulation of outer membrane proteins and virulence determinants in *Vibrio cholerae* requires *toxR*. J. Bacteriol. **170:**2575–2583.
42. **Ochs, M., S. Veitinger, I. Kim, D. Welz, A. Angerer, and V. Braun.** 1995. Regulation of citrate-dependent iron transport of *Escherichia coli*: FecR is required for transcription activation by FecI. Mol. Microbiol. **15:**119–132.
43. **Pendrak, M. L., and R. D. Perry.** 1993. Proteins essential for expression of the Hms^+ phenotype of *Yersinia pestis*. Mol. Microbiol. **8:**857–864.
44. **Perry, R. D.** 1993. Acquisition and storage of inorganic iron and hemin by the yersiniae. Trends Microbiol. **1:**142–147.
45. **Perry, R. D., and R. R. Brubaker.** 1979. Accumulation of iron by yersiniae. J. Bacteriol. **137:**1290–1298.
46. **Perry, R. D., M. L. Pendrak, and P. Schuetze.** 1990. Identification and cloning of a hemin storage locus involved in the pigmentation phenotype of *Yersinia pestis*. J. Bacteriol. **172:**5929–5937.
47. **Pospeich, A., B. Cluzel, J. Bietenhader, and T. Schupp.** 1995. A new *Myxococcus xanthus* gene cluster for the biosynthesis of the antibiotic saframycin Mx1 encoding a peptide synthetase. Microbiology **141:**1793–1803.
48. **Rakin, A., E. Saken, D. Harmsen, and J. Heesemann.** 1994. The pesticin receptor of *Yersinia enterocolitica*: a novel virulence factor with dual function. Mol. Microbiol. **13:**253–263.
49. **Reed, L. J., and H. Muench.** 1938. A simple method of estimating fifty per cent endpoints. Am. J. Hyg. **27:**493–497.
50. **Rusnak, F., M. Sakaitani, D. Drueckhammer, J. Reichert, and C. T. Walsh.** 1991. Biosynthesis of the *Escherichia coli* siderophore enterobactin: sequence of the *entF* gene, expression and purification of EntF, and analysis of covalent phosphopantetheine. Biochemistry **30:**2916–2927.
51. **Sambrook, J., E. F. Fritsch, and T. Maniatis.** 1989. Molecular cloning: a laboratory manual, 2nd ed. Cold Spring Harbor Laboratory Press, Cold Spring Harbor, N.Y.
52. **Sanger, F., S. Nicklen, and A. R. Coulson.** 1977. DNA sequencing with chain-terminating inhibitors. Proc. Natl. Acad. Sci. USA **74:**5463–5467.
53. **Schlumbohm, W., T. Stein, C. Ullrich, J. Vater, M. Krause, M. A. Maraheil, V. Kruft, and B. Wittmann-Liebold.** 1991. An active serine is involved in covalent substrate amino acid binding at each reaction center of gramicidin S synthetase. J. Biol. Chem. **266:**23135–23141.
54. **Sikkema, D. J., and R. R. Brubaker.** 1987. Resistance to pesticin, storage of iron, and invasion of HeLa cells by yersiniae. Infect. Immun. **55:**572–578.
55. **Sikkema, D. J., and R. R. Brubaker.** 1989. Outer membrane peptides of *Yersinia pestis* mediating siderophore-independent assimilation of iron. Biol. Metals **2:**174–184.
56. **Southern, E. M.** 1975. Detection of specific sequences among DNA fragments separated by gel electrophoresis. J. Mol. Biol. **98:**503–517.
57. **Staab, J. F., M. F. Elkins, and C. F. Earhart.** 1989. Nucleotide sequence of the *Escherichia coli entE* gene. FEMS Microbiol. Lett. **50:**15–19.
58. **Staggs, T. M., and R. D. Perry.** 1991. Identification and cloning of a *fur* regulatory gene in *Yersinia pestis*. J. Bacteriol. **173:**417–425.
59. **Staggs, T. M., and R. D. Perry.** 1992. Fur regulation in *Yersinia* species. Mol. Microbiol. **6:**2507–2516.
60. **Straley, S. C., and W. S. Bowmer.** 1986. Virulence genes regulated at the transcriptional level by Ca^{2+} in *Yersinia pestis* include structural genes for outer membrane proteins. Infect. Immun. **51:**445–454.
61. **Surgalla, M. J., and E. D. Beesley.** 1969. Congo red-agar plating medium for detecting pigmentation in *Pasteurella pestis*. Appl. Microbiol. **18:**834–837.
62. **Tartof, K. D., and C. A. Hobbs.** 1987. Improved media for growing plasmid and cosmid clones. Focus **9:**12.
63. **Tognoni, A., E. Franchi, C. Magistrelli, E. Colombo, P. Cosmina, and G. Grandi.** 1995. A putative new peptide synthase operon in *Bacillus subtilis*: partial characterization. Microbiology **141:**645–648.
64. **Vieira, J., and J. Messing.** 1982. The pUC plasmids, an M13mp7-derived system for insertion mutagenesis and sequencing with synthetic universal primers. Gene **19:**259–268.
65. **Wake, A., M. Misawa, and A. Matsui.** 1975. Siderochrome production by *Yersinia pestis* and its relation to virulence. Infect. Immun. **12:**1211–1213.

Editor: A. O'Brien